Nitric Oxide 84 (2019) 30–37

Contents lists available at ScienceDirect

Nitric Oxide

journal homepage: www.elsevier.com/locate/yniox

Long-term decomposition of aqueous S-nitrosoglutathione and S-nitroso-N-acetylcysteine: Influence of concentration, temperature, pH and light

Gabriela Freitas P. de Souza[1], Jaqueline Priscilla Denadai[1], Guilherme F. Picheth, Marcelo Ganzarolli de Oliveira*

Institute of Chemistry, University of Campinas, UNICAMP, Campinas, SP, Brazil

ARTICLE INFO

Keywords:
S-nitrosothiols
S-nitrosoglutathione
S-nitroso-N-acetylcysteine
Nitric oxide
Long-term stability

ABSTRACT

Primary S-nitrosothiols (RSNOs) have received significant attention for their ability to modulate NO signaling in many physiological and pathophysiological processes. Such actions and their potential pharmaceutical uses demand a better knowledge of their stability in aqueous solutions. Herein, we investigated the effects of concentration, temperature, pH, room light and metal ions on the long-term kinetic behavior of two representative primary RSNOs, S-nitrosoglutathione (GSNO) and S-nitroso-*N*-acetylcysteine (SNAC). The thermal decomposition of GSNO and SNAC were shown to be affected by the auto-catalytic action of the thiyl radicals. At 25 °C in the dark and protected from the catalytic action of metal ions, GSNO and SNAC solutions 1 mM showed half-lives of 49 and 76 days, and apparent activation energies of 84 ± 14 and 90 ± 6 kJ mol^{-1}, respectively. Both GSNO and SNAC exhibited increased stability in the pH range 5–7. At high pH the decomposition pathway of GSNO involves the formation of an intermediate (GS-NO_2^{2-}), which decomposes generating GSH and nitrite. GSNO solutions displayed lower sensitivity to the catalytic action of metal ions than SNAC and the exposure to room light led to a 5-fold increase in the initial rates of decomposition of both RSNOs. In all comparisons, SNAC solutions showed higher stability than GSNO solutions. These findings provide strategic information about the stability of GSNO and SNAC and may open new perspectives for their use as experimental or therapeutic NO donors.

1. Introduction

The multiple physiological and pathophysiological roles played by nitric oxide (NO) have fostered a continuous investigation on the behavior of NO donors. In spite of the existence of different classes of synthetic molecules capable of directly releasing NO (e.g. metal-nitrosyl complexes [1] and diazeniumdiolates (NONOates) [2]), primary S-nitrosothiols have received a significant amount of attention due to their role as endogenous NO carriers in mammals and their ability to deliver NO locally [3–6].

S-nitrosoglutathione (GSNO) and S-nitroso-N-acetylcysteine (SNAC) (Fig. 1), in particular, have been investigated for their ability to act as exogenous NO donors in several pharmaceutical formulations [7–10]. GSNO and SNAC can be synthesized through the S-nitrosation of glutathione (GSH) and N-acetylcysteine (NAC), respectively, by nitrous acid (HONO) or dinitrogen trioxide (N_2O_3) [11–13]. Several reports have shown that GSNO is an effective NO donor which displays beneficial actions in topical applications for increasing dermal vasodilation [12] accelerating wound healing [14–18] and promoting analgesic action [19]. SNAC, in turn, have been shown to exert several potential therapeutic actions, including the lowering of blood pressure [20], the prevention of early plaque development [8], the prevention and reversion of steatohepatitis [21–23], the attenuation of liver fibrosis [24], the amelioration of ischemia/reperfusion injury in steatotic liver [25], the killing of leishmania [26] and trophozoites of *Acanthamoeba castellanii* [27] and the enhancement of gastric mucosal blood flow [9]. Its precursor, NAC, has a wide use as a pharmaceutical compound and is considered to be a prodrug for L-cysteine, whose oral administration has been used for increasing GSH biosynthesis [28].

In practical situations, the stability of aqueous RSNOs solutions is subjected to the effects of concentration, pH and temperature. room light [29–34]. In addition, primary and tertiary RSNOs also undergo photodecomposition under exposure to UV or visible light [35] and are sensitive to the catalytic actions of trace metal ions (specially Cu(II) ions) [36–38], and N_2O_3 in aerobic conditions [39,40].

In the absence of metal ions and light, the basic decomposition

* Corresponding author.
E-mail address: mgo@unicamp.br (M.G. de Oliveira).
[1] These authors contributed equally.

https://doi.org/10.1016/j.niox.2019.01.002
Received 5 October 2018; Received in revised form 17 November 2018; Accepted 4 January 2019
Available online 07 January 2019
1089-8603/

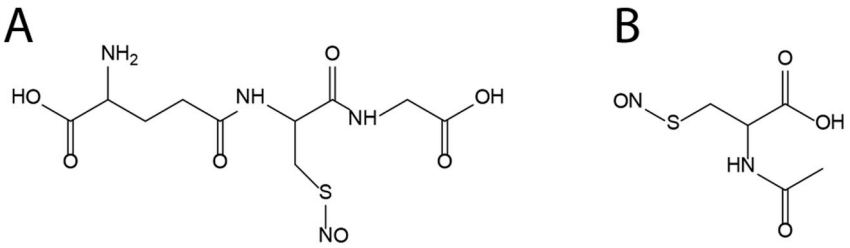

Fig. 1. Structures of S-nitrosoglutathione, GSNO (A) and S-nitroso-N-acetylcysteine, SNAC (B).

pathway of primary RSNOs in aqueous solutions is a bimolecular reaction, which produces free NO and dimers bonded by disulfide linkages as represented in the general Eq. (1).

$$2RSNO \rightarrow RS\text{-}SR + 2NO \quad (1)$$

The pH effect on the stability of aqueous RSNOs is claimed to involve the equilibrium between the two resonance structures of Eq. (2) [41–43]:

$$RSN = O_{(I)} \leftrightarrows RS^{+} = NO^{-}_{(II)} \quad (2)$$

In acidic medium, the oxygen atom of structure II is protonated contributing to an increased strength of the S—N, bond, and thereby an increased stability. The homolytic S—N bond cleavage is also susceptible to the autocatalytic action of the thiyl radicals (RS·) as previously reported [34] (Eqs. (3)–(5)).

$$RSNO \rightarrow RS\cdot + NO\cdot \quad (3)$$

$$RS\cdot + RSNO \rightarrow RS\text{-}SR + NO \quad (4)$$

$$2\ RS\cdot \rightarrow RS\text{-}SR \quad (5)$$

The spontaneous decomposition of aqueous GSNO and SNAC, subjected to the above-mentioned factors, may impose important limitations for their storage and use as experimental NO donors and for therapeutic purposes. We have reported several strategies to overcome these limitations based on the incorporation of GSNO and SNAC into hydrophilic polymeric matrices such as the triblock copolymer poly(ethylene oxide)$_{99}$-poly(propylene oxide)$_{69}$-poly(ethylene oxide)$_{99}$, Pluronic-F127 [18,44], hydroxypropylmethyl cellulose (HPMC) [45], poly(ethylene glycol) [13], poly(vinylpyrrolidone) [46] and poly(vinyl alcohol) [35,47,48]. However, such studies were limited to time scales of hours and the characterization of the long-term stabilities of aqueous GSNO and SNAC solutions is still lacking. In this study we characterized the effects of concentration, temperature, pH and room light on the kinetic behavior of aqueous GSNO and SNAC solutions over storage periods ranging from 7 to 80 days. The results obtained provide insights into the different decomposition pathways which may operate in these RSNOs under specific conditions and may broaden the perspectives for the use GSNO and SNAC as experimental or therapeutic NO donors.

2. Materials and methods

2.1. Reagents

Glutathione (Glu-Cys-Gly, GSH), N-acetylcysteine (NAC), sodium nitrite, EDTA, benzalkonium chloride, sodium phosphate (Na_2HPO_4), citric acid, glycine and sodium hydroxide (NaOH) (Sigma, St. Louis, MO, USA) were used as received. All the experiments were carried out using analytical grade water from a Millipore Milli-Q Gradient filtration system (conductivity 18.2 MΩ cm at 25 °C).

2.2. GSNO and SNAC synthesis

S-nitrosoglutathione (GSNO) was synthesized by the S-nitrosation of GSH in acidic sodium nitrite solution as previously described [24]. Briefly, reduced glutathione was reacted with an equimolar amount of sodium nitrite in aqueous HCl solution 0.5 M. The product was precipitated in cold acetone, vacuum-filtered, washed with cold acetone, freeze-dried during 24 h and stored in a desiccator containing anhydrous silica gel at 25 °C, protected from light. Aqueous SNAC stock solution was prepared as reported by de Souza et al. [26] by reacting equimolar (1.0×10^{-2} mol L^{-1}) solutions of NAC and sodium nitrite under stirring at room temperature for 15 min protected from light. SNAC solutions were used immediately after synthesis. Unless otherwise stated, GSNO and SNAC solutions were prepared in 0.09 M phosphate buffer solution pH 7.0 with 3.4 mM (0.1% w/w) of EDTA, 0.6 mM (0.02% w/w) of benzalkonium chloride (added as a preservative agent to inhibit microbial proliferation during the incubation times) and kept in the dark at 25 °C. The final concentrations of GSNO and SNAC were assessed by UV–vis spectrophotometry using the characteristic absorption bands of RSNOs at λ = 336 nm ($n_O \rightarrow \pi^*$ electronic transition, $\varepsilon = 922\ M^{-1}\ cm^{-1}$) and λ = 545 nm ($n_N \rightarrow \pi^*$ electronic transition, $\varepsilon = 16\ M^{-1}\ cm^{-1}$) ([35,49], Fig. S1).

2.3. Kinetic monitoring of GSNO and SNAC decomposition

The spectral changes of GSNO and SNAC solutions were monitored in the range 220–1100 nm in the dark, referenced against air, using a diode array spectrophotometer (Hewlett–Packard, Model 8453, Palo Alto, CA, USA). GSNO and SNAC solutions were kept in closed vials inside a thermostatic bath at the desired temperature. Aliquots were collected from these vials at selected times, and the kinetic curves of GSNO and SNAC decomposition were obtained from the absorption changes measured at λ = 336 or 545 nm. Quartz cuvettes with optical paths 0.1, 0.5 and 1.0 cm were used to assure starting absorption values in the range of 0.5–1 in the kinetic monitoring (Table S1).

The fast decomposition of GSNO and SNAC solutions at pH 13 and of SNAC in the absence of EDTA were monitored directly in quartz cuvettes inserted in the temperature-controlled sample holder of the spectrophotometer in time intervals of 10–15 min during 4 h for SNAC and 24 h for GSNO. The absorbance at 336 or 545 nm versus time curves were normalized (dividing by the initial absorbance value) in order to correct for small differences in the starting concentration of the solutions. The initial rates (I_R) of GSNO and SNAC decomposition were obtained from linear regression of the initial sections (less than 10% of the reaction extent) of the kinetic curves, according to Eq. (6):

$$I_R = \Delta(RSNO)/\Delta t, \quad (6)$$

where Δ(RSNO) is the change in the RSNO absorbance and Δt is the corresponding time interval.

The kinetic curves of RSNO decomposition were fitted to a first order exponential decay using the software Origin® and the first order rate constants (k) were calculated. Each point in the kinetic curves represents the average of three independent measurements, with the error bars expressed by their standard error of the mean (SEM).

2.4. Concentration effect on the kinetics of GSNO and SNAC decomposition

The absorbance of GSNO and SNAC solutions was monitored in

seven different concentrations: 1, 2, 5, 10, 20, 40 and 50 mM in the presence of EDTA 0.1 wt% at 25 °C in PBS solution, pH 7.0 and the *k* and I_R values were extracted from the kinetic curves.

2.5. Temperature effect on the kinetics of GSNO and SNAC decomposition

GSNO and SNAC solutions (1 mM) were placed in 25-mL glass vials maintained at 15 °C, 25 °C, 30 °C, 35 °C e 40 °C in thermostatic baths and spectrophotometrically monitored according to the above-described procedure. The apparent activation energies (E_a) for the thermal cleavage of the S—N bond of GSNO and SNAC were estimated from Arrhenius plots of ln I_R versus 1/T. The thermal decomposition of GSNO and SNAC solutions (1 mM) at 40 °C were also studied in the absence of EDTA in order to evaluate the catalytic effect of trace metal ions present in the reactants and water on the reactions. The effect of EDTA on the stability of GSNO and SNAC solutions (1 mM) was evaluated at 40 °C (pH 7.0) with or without EDTA (0.1 wt%).

2.6. pH effect on the kinetics of GSNO and SNAC decomposition

The pH effect on the GSNO and SNAC decomposition was analyzed in the pH range 3–13. The required pH values were obtained using buffer solutions of Na_2HPO_4/citric acid (pH 3, 5 and 7) and glycine/NaOH (pH 9, 11 and 13) at 25 °C. The GSNO and SNAC solutions (1 mM) at the above-mentioned pH values were prepared by dissolving solid GSNO or diluting stock SNAC solution (50 mM) in the corresponding buffer solutions. The pH values of the solutions were measured with a micro pH electrode and a pH meter (Denver Instruments, Arvada, Colorado, USA).

2.7. Nitrite quantification

The generation of nitrite (NO_2^-) ions in the decomposition of GSNO at pH 13 was characterized by selectively reducing NO_2^- to NO with ascorbic acid, followed by NO detection and quantification by ozone-based chemiluninescence using a NO Analyzer (NOA 280i, Sievers) operating at 6.0 psig of O_2 and 7.0 Torr of N_2 [50]. After the beginning of the decomposition of GSNO solution at pH 13 (carried out in a vial with a rubber septum), aliquots of 4 µL were extracted from this solution every 15 min and injected in the reaction flask of the NOA, during 2 h, which is the time necessary for the complete vanishing of the absorption band of GSNO at 336 nm at pH 13. A calibration curve for NO_2^- was obtained in the range of 12.5–500 µmol L^{-1} using a standard sodium nitrite solution.

2.8. Light-induced decomposition of GSNO and SNAC solutions

SNAC and GSNO solutions 1 mM were placed in 25 mL glass vials and continuously exposed to room light for evaluating their photochemical decomposition. Control experiments were performed under the same conditions with the vials protected from light with aluminum foil. Room light intensity on the top of the laboratory bench was measured at the wavelengths 336 and 545 nm using a radiometer Cole Parmer H-97503. The readings at these wavelengths were 55 and 41.5 µW cm^{-2}, respectively.

3. Results and discussion

3.1. Synthesis of GSNO and SNAC

GSNO and SNAC were synthesized through the S-nitrosation reactions of the parent sulphydril-containing GSH and NAC by acidified nitrite. Under acidic conditions, nitrite is protonated yielding nitrous acid (HO—NO). The nitrosonium cation (NO^+) present in the charge-separation structure of HO—NO performs a nucleophilic attack on the sulfur atom of the sulphydryl (—SH) group, followed by the elimination of a water molecule, leading to the formation of the S-nitrosothiol moiety, according to the following general equations:

$$NO_2^- + H^+ \rightarrow HNO_2 = HO^{\delta-}—NO^{\delta+} \quad (7)$$

$$HO^{\delta-}—NO^{\delta+} + RSH \rightarrow RSNO + H_2O \quad (8)$$

The formation of GSNO and SNAC in the S-nitrosation of GSH and NAC, respectively, were confirmed by their characteristic absorption bands at 545 and 336 nm. The stabilizing effect of EDTA on the decomposition of GSNO and SNAC was confirmed by comparing their decomposition profiles under accelerated thermal decomposition condition (40 °C). The significant reduction in the decomposition rates of both GSNO and SNAC in the presence of EDTA (Fig. S2) is in accordance with other reports on the catalytic action of trace copper ions on the thermal decomposition of RSNOs [51]. Therefore, the kinetic behavior of GSNO and SNAC solutions in all the other experiments of the presence study was characterized in the presence of EDTA 0.1 wt%.

3.2. Concentration effect on GSNO and SNAC decomposition

We have previously reported that the thermal decomposition of aqueous S-nitrosocysteine (CysNO), SNAC and GSNO solutions is subjected to an autocatalytic effect, which is reflected in increased rate constants of decay with increasing initial concentration [34]. This effect was assigned to the secondary bimolecular reactions between the thiyl radicals, formed in the primary homolytic cleavage of the S—N bond of the S—NO group and intact RSNO molecules, which leads to the formation of S—S bonded dimers and further free NO release. The second possible fate of the thiyl radicals is dimerization with another thiyl radical. Therefore, the higher the rate of primary production of thiyl radicals, the higher is their autocatalytic action on intact RSNO molecules (Fig. 2). In addition, the geminate recombination of the NO· and RS· radicals is also subjected to the cage effect of the solvent [13,52]. Since, at the beginning of the reaction, the concentration of intact RSNO molecules is much higher than the concentration of thiyl radicals, the kinetic behavior of the decomposition reactions follows, in general, a pseudo-first order law.

To evaluate the long-term concentration effect on the thermal decomposition profiles of GSNO and SNAC solutions, we monitored their decompositions in the concentration range of 1–50 mM at 25 °C, protected from light, at pH 7 for 80 days. The kinetic curves obtained are shown in Fig. 3 A and B. These curves were fitted to first order decay equations, from which the pseudo-first order *k* values and the corresponding half-lives ($t_{1/2}$) were extracted (Table S3, Fig. 3C). It can be seen that *k* values increase consistently with the increase in the initial concentration for both GSNO and SNAC solutions. At low initial concentrations (1–2 mM), the decomposition pathway is expected to be governed by the primary spontaneous homolytic cleavage of the S—N

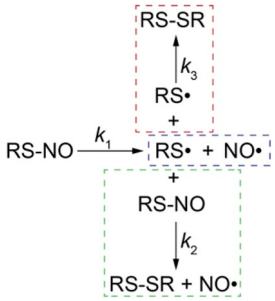

Fig. 2. General mechanism of primary RSNOs thermal decomposition showing the formation of thiyl radical and free NO in a primary process (K_1), followed by secondary reactions that may involve the bimolecular reactions between the thiyl radical and an intact RSNO molecule (autocatalytic reaction, K_2) or between two thiyl radical (K_3), leading in both cases to the formation of S-S bound dimers.

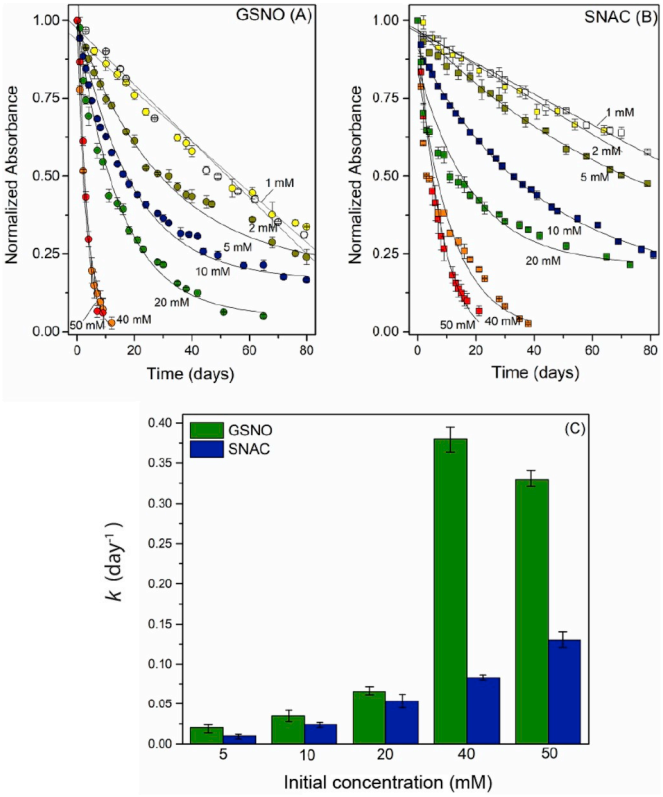

Fig. 3. Kinetic curves of decomposition of aqueous GSNO (A) and SNAC (B) solutions and first order rate constants (k) (C) in the concentration range of 1–50 mM. All solutions were maintained at 25 °C protected from light at pH 7 in the presence of EDTA 0.1 wt%. For the spectrophotometric monitoring conditions used see Table S1.

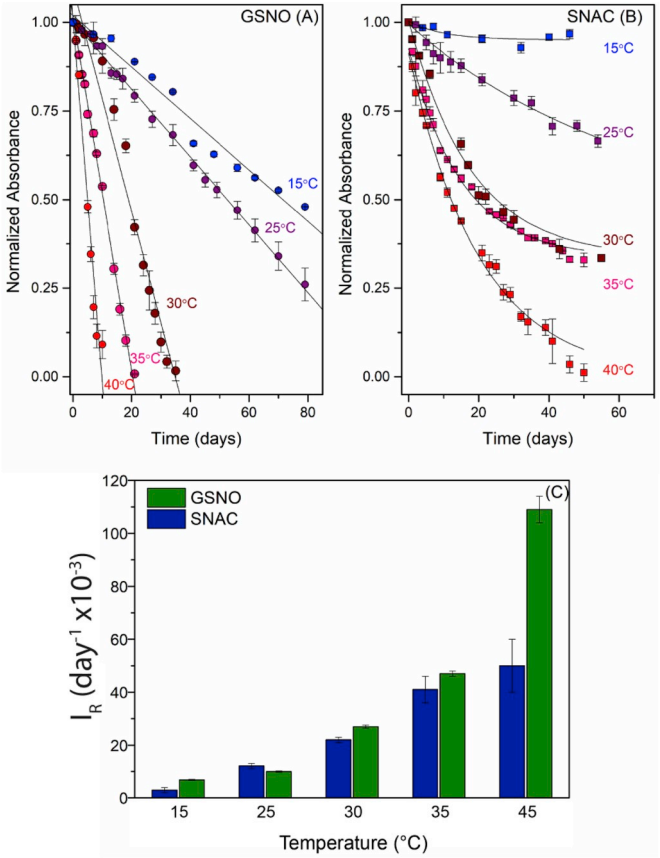

Fig. 4. Kinetic curves of decomposition of aqueous GSNO (A) and SNAC (B) solutions 1 mM and initial decomposition rates (I_R) (C) in the temperature range of 15 to 45 °C. All solutions were maintained at 25 °C protected from light at pH 7 in the presence of EDTA 0.1 wt%. Absorbance measurements based on the decay of the absorption band with maximum at 336 nm.

bond, so relatively low k values are obtained compared with the decompositions at higher initial concentrations, where the autocatalytic effect of the thiyl radicals operate, promoting a parallel reaction with intact RSNO molecules.

It can also be seen that in all cases GSNO led to higher k values than SNAC. Doubling the GSNO concentration from 5 to 10 mM and from 10 to 20 mM, led to 1.8 and 1.9-fold increases in k, respectively. No significant difference was observed between the k values of GSNO 40 and 50 mM, probably due to the lower quality of the curve fittings at these concentrations. Doubling the SNAC concentration from 5 to 10 mM and from 10 to 20 mM led to 2.4 and 2.3-fold increases in k, respectively and a further 1.5-fold increase in k was observed with the increase in the initial concentration from 40 to 50 mM. Overall, these results show that while both RSNOs are subjected to the autocatalytic effect of concentration, GSNO is more sensitive to this effect than SNAC.

The higher intrinsic stability of SNAC compared to GSNO is likely to be associated with the establishment of an intramolecular hydrogen bond between the carbonylic oxygen atom of the acetamido group (−NHCOCH$_3$) and the hydrogen atom of the protonated carboxylic group of the molecule, leading to the formation of a stable seven-membered ring (−H−O−C−C−N−C−O−) and to an increase in the strength of the S−N bond, as we reported before [34].

3.3. Temperature effect on the GSNO and SNAC decomposition

The long-term temperature dependence of the thermal decomposition reactions of GSNO and SNAC solutions 1 mM in the temperature range of 15–40 °C are shown in the kinetic curves of Fig. 4 A and B, respectively. A significant increase in the rate of decomposition is observed for both GSNO and SNAC with the increase in temperature. Although, in both cases, the kinetics is expected to be governed by the primary unimolecular S−N bond cleavage reaction, the faster decay of GSNO at all temperatures did not allow curve fittings to a first-order exponential decay. Therefore, a comparative analysis in this case was performed using the I_R values of reactions, as described in Eq. (6) (Table S4 and Fig. 4C).

It can be seen that the increments in the I_R values with the increase in temperature are similar for GSNO and SNAC in the temperature range of 15–35 °C, while at 40 °C the I_R of GSNO decomposition is 2.2-fold higher than the I_R of SNAC. The apparent Arrhenius activation energies (E_a) of the decomposition reactions, calculated on the bases of the I_R values in both cases, led to similar E_a for GSNO and SNAC: 84 ± 14 and 90 ± 6 kJ mol^{-1}, respectively. These E_a values have the same order of magnitude of the value reported elsewhere for GSNO (60.5 ± 4 kJ mol^{-1}) [53], obtained in the absence of EDTA and pH control. The relatively high E_a values obtained are also in accordance with results reported by Bartberger et al. [54]. Based on computed free energy of activation for the homolysis of primary RSNOs, these authors predicted a half-life with respect to the S−N bond cleavage of 2.1 years at 37 °C. This prediction led to the conclusion that these kinetic parameters are too high and prohibitive for considering that the homolytic cleavage mechanism operates for RSNOs under physiological conditions. Our results reinforce this conclusion and allow suggesting that other mechanisms, (e.g. transnitrosation across cell membranes) are involved in the transfer of NO from circulating primary RSNOs to other target molecules, in line with other reports [55–58].

The higher thermal stability of SNAC compared to GSNO is in accordance with its higher stability regarding the auto-catalytic effect of concentration shown in Fig. 3. Again, this difference may be associated

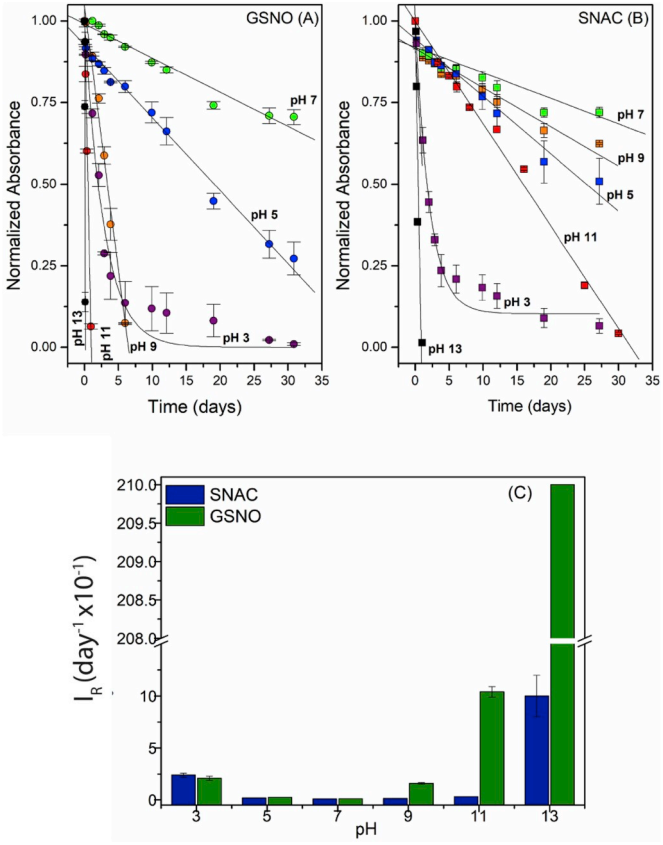

Fig. 5. Kinetic curves of decomposition of aqueous GSNO (A) and SNAC (B) solutions 1 mM and initial decomposition rates (I_R) (C) in the pH range of 3–13. All solutions were maintained at 25 °C protected from light at pH 7 in the presence of EDTA 0.1 wt%. Absorbance measurements based on the decay of the absorption band with maximum at 336 nm.

with the increased stability conferred to SNAC by the intramolecular hydrogen bonding involving the acetamido and carboxylic acid groups, as discussed above. Overall, these results show that both GSNO and

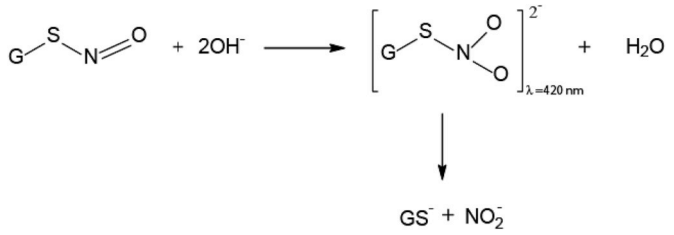

Fig. 7. Schematic representation of the mechanism of GSNO decomposition in basic medium (pH 13).

SNAC solutions 1 mM can be considered quite stable at 15 °C. In fact, SNAC decomposition over a period of 50 days at 15 °C is not significant, opening perspectives for its broader use as an experimental NO donor molecule.

3.4. pH effect on the GSNO and SNAC decomposition

To assess the long-term pH effect on the decomposition pathways of GSNO and SNAC solutions, their kinetic behaviors were studied in the pH range of 3–13 over 30 days. The kinetic curves obtained are shown in Fig. 5 A and B. It can be seen that pH lower than 5 and higher than 9, significantly increase the rate of decomposition of both GSNO and SNAC. Interestingly, the rates of decomposition were the lowest around the neutral physiological pH and was greatly increased at pH 11 and 13, specially for GSNO. Except for the data obtained at pH 3, which could be fitted to first-order exponential decays, the straight lines of Fig. 5 A and B were obtained by linear regression of the data and were used to calculate the I_R values of the reactions. These values (including the I_R for the initial sections of the curves at pH 3) are shown in Fig. 5C and Table S5, which also shows the estimated $t_{1/2}$ values of reactions in each case. As can be seen, the $t_{1/2}$ values at pH 7 are surprisingly long (50.4 days and 46.2 days for GSNO and SNAC, respectively) having the same order of magnitude of those obtained for the SNAC solutions 1 mM at pH 7.0 at 25 °C (Table S4). In a physiological point of view, the increased stability at pH 7 is in accordance with the fact that GSNO is identified as an endogenous NO carrier capable of transporting NO in the plasma to distant targets [59,60]. In this respect, it calls attention that SNAC is even more stable than GSNO in a wider pH range with

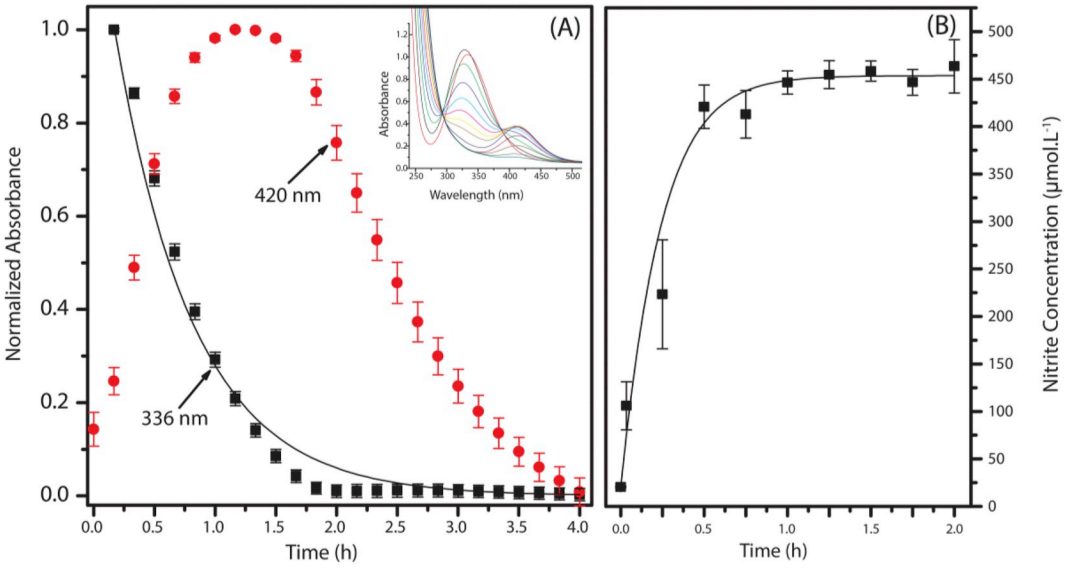

Fig. 6. Kinetic curves corresponding to the spectral changes (inset) monitored at 336 and 420 nm during the decomposition of GSNO 1 mM at pH 13 (A). Kinetic curve of nitrite formation in the GSNO decomposition at pH 13, quantified by chemiluminescence (B). The experiments were performed in the dark with EDTA 0.1 wt % at 25 °C.

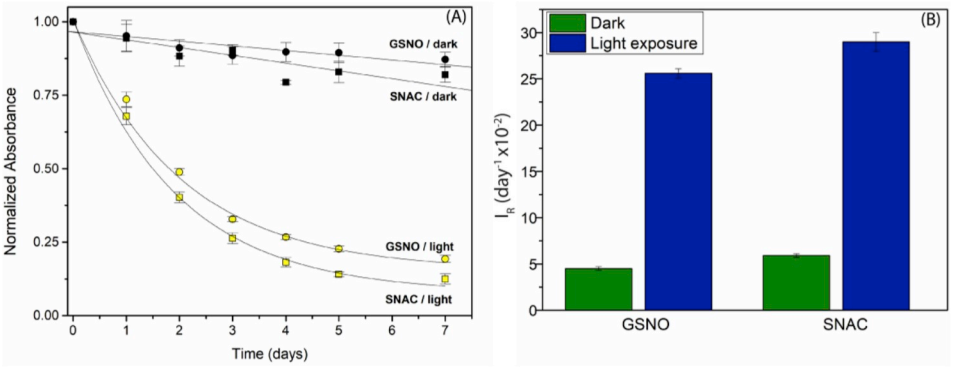

Fig. 8. Kinetic curves of decomposition of aqueous GSNO and SNAC solutions 1 mM in the presence of EDTA 0.1 wt% at 25 °C and pH 7 in the dark and under room light exposure (A) and corresponding initial rates of decomposition (B). Absorbance measurements based on the decay of the absorption band with maximum at 336 nm.

GSNO/SNAC decomposition ratios of 13.4, 33.5 and 21 at pH 9, 11 and 13, respectively. These results differ from the those reported by by Heikal et al. [42] who showed higher GSNO stability at pH 4 up to 3 h. However, it must be considered that the long-term monitoring herein shown may reveal differences in the kinetic behavior of the RSNOs, which cannot be evaluated in short-term monitoring.

To further investigate the fast GSNO decomposition at pH 13, we monitored its decomposition at this pH spectrophotometrically, with data acquisition every 10 min, during 4 h. In addition to the exponential decay of the absorption band of GSNO at 336 nm, this monitoring revealed a transient band with maximum at 420 nm, which starts appearing as soon as GSNO is exposed to the pH 13.

The maximum of this transient band is reached after 2 h, and after 4 h it is completely bleached (Fig. 6A). A parallel monitoring of this reaction for the detection and quantification of nitrite (NO_2^-) by chemiluminescence revealed a continuous formation of NO_2^- with maximum achieved after 2 h, hence, correlated with the full bleaching of the transient band at 420 nm (Fig. 6B). These spectral changes suggest that an intermediary nitrated species is responsible for the transient band at 420 nm. It has already been reported that the degradation of RSNOs in basic medium may involve a nucleophilic attack of the hydroxyl anion (OH^-) on the nitrogen atom of the nitrosyl group [38], yielding an intermediate ($RS\text{-}NO_2^{2-}$) Based on the correlation between the bleaching of this transient band and the evolution of the NO_2^- concentration, we assigned this transient band to the ($GS\text{-}NO_2^-$) intermediate, which undergoes further decomposition yielding the parent GS^- thiolate anion and NO_2^- (Fig. 7).

A similar nucleophilic attack of the OH^- anion on the nitrosyl group, followed by NO_2^- formation, was reported for the decomposition of sodium nitroprusside in basic medium [61]. In fact, the susceptibility of RSNOs to the nucleophile attack of other species (e.g. SO_3^{2-}, S_2^{2-} and H_2O_2) has also been reported and can take place at pH just below 7, such as in acidosis condition [38,62].

The fast decomposition of GSNO in basic medium can therefore be assigned mainly to the above-described mechanism. Although in the case of SNAC, the formation of the intermediary nitrated species could not be observed, it is likely that the same mechanism operates in its decomposition in basic medium.

The increased rates of GSNO and SNAC decomposition at pH 3 are much less pronounced than at high pH as can be seen in Fig. 5. As reported by Moran et al. [43], at pH values lower than 7, GSNO and SNAC undergo acid-catalyzed hydrolysis due to the protonation of the sulfur atom of the S—NO group, thus facilitating the nucleophilic attack by the oxygen atom of the water molecule on the nitrogen atom of the NO group, generating an intermediary complex ($[RS—NO]^+$), which undergoes hydrolysis producing the parent thiol.

Further studies should address the relative contribution of this mechanistic pathway, compared to the bimolecular dimerization pathway (Eq. (1)).

3.5. Room light effect of the GSNO and SNAC decomposition

Fig. 8 shows the kinetic curves of decomposition of GSNO and SNAC solutions 1 mM at 25 °C in the dark and under room light exposure, during 7 days. It can be seen that room light at an intensity normally found over laboratory benches, leads to a 5-fold increase in the initial rates of decomposition of both GSNO and SNAC, compared with the rates observed in the dark. This acceleration is explained by the excitation of the photoactive absorption bands of primary RSNOs at 336 and 550 nm, which populate the π^* anti-bonding orbital of the SNO group, weakening the S—N bond and leading to NO ejection, as already reported elsewhere [35,63]. The present results highlight the importance of protecting aqueous RSNOs solutions from room light during all the laboratory procedures.

4. Conclusions

GSNO and SNAC solutions are subjected to the autocatalytic effect of the thiyl radicals formed in the primary homolytic S—N bond cleavage, which is much more pronounced for GSNO than for SNAC at concentrations above 20 mM. GSNO and SNAC solutions undergo thermal decomposition in the dark with apparent Arrhenius activation energies of 84 ± 14 and 90 ± 6 kJ mol^{-1}, respectively. SNAC stability is not affected by the pH in the pH range of 5–11. Both RSNOs are slightly less stable in acidic medium up to pH 3, while their decomposition rates are greatly increased above pH 11 for GSNO and pH 13 for SNAC. The accelerated GSNO decomposition in basic medium is associated with the formation of a transient nitrated species ($GSNO_2^{2-}$), which undergoes decomposition, forming GSH and nitrite. Both GSNO and SNAC solutions are similarly sensitive to normal room light, which reduces their half-lives from 1.2 to 0.57 days. At concentrations equal or below 1 mM, in the pH range of 5–9, in the presence of a metal chelator and protected from light, GSNO and SNAC solutions can be considered quite stable and SNAC solution, in particular, can be stored over more than one month at 15 °C with negligible decomposition.

Acknowledgments

GFPS, JPD and GFP received fellowships from the São Paulo Research Foundation (FAPESP) (grants 07/55877-3, 07/50995-8 and 17/19253-7, respectively). MGO acknowledges FAPESP [grant number 16/02414-5] for financial support.

Appendix A. Supplementary data

Supplementary data to this article can be found online at https://doi.org/10.1016/j.niox.2019.01.002.

References

[1] L. Li, L. Li, Recent advances in multinuclear metal nitrosyl complexes, Coord. Chem. Rev. 306 (2016) 678–700.
[2] M.M. Reynolds, Z. Zhou, B.K. Oh, M.E. Meyerhoff, Bis-diazeniumdiolates of dialkyldiamines: enhanced nitric oxide loading of parent diamines, Org. Lett. 7 (2005) 2813–2816.
[3] N. Hogg, The biochemistry and physiology of S-nitrosothiols, Annu. Rev. Pharmacol. Toxicol. 42 (2002) 585–600.
[4] N. Hogg, K.A. Broniowska, J. Novalija, N.J. Kettenhofen, E. Novalija, Role of S-nitrosothiol transport in the cardioprotective effects of S-nitrosocysteine in rat hearts, Free Radic. Biol. Med. 43 (2007) 1086–1094.
[5] K.A. Broniowska, A.R. Diers, N. Hogg, S-nitrosoglutathione, Biochim. Biophys. Acta Gen. Subj. 1830 (2013) 3173–3181.
[6] R.P. Patel, S. Yuan, C.G. Kevil, S-nitrosothiols and nitric oxide biology, in: L.J. Ignarro, B.A. Freeman (Eds.), Nitric Oxide: Biology and Pathobiology, Elsevier, London, 2017, pp. 45–56.
[7] M.G. de Oliveira, S-Nitrosothiols as platforms for topical nitric oxide delivery, Basic Clin. Pharmacol. Toxicol. 119 (2016) 49–56.
[8] M. Krieger, K. Santos, S. Shishido, A. Wanschel, H. Estrela, L. Santos, M.G. de Oliveira, K. Franchini, R. Spadari-Bratfisch, F. Laurindo, Antiatherogenic effects of S-nitroso-N-acetylcysteine in hypercholesterolemic LDL receptor knockout mice, Nitric Oxide 14 (2006) 12–20.
[9] G.F. de Souza, P. Taladriz-Blanco, L.A. Velloso, M.G. de Oliveira, Nitric oxide released from luminal S-nitroso-N-acetylcysteine increases gastric mucosal blood flow, Molecules 20 (2015) 4109–4123.
[10] W. Andraus, G.F.P. de. Souza, M.G. de Oliveira, L.B. Haddad, A.M.M. Coelho, F.H. Galvão, R.M.C. Leitão, L.A.C. D'Albuquerque, M.C.C. Machado, S-nitroso-N-acetylcysteine ameliorates ischemia-reperfusion injury in the steatotic liver, Clinics 65 (2010) 715–721.
[11] N.J. Kettenhofen, K.A. Broniowska, A. Keszler, Y. Zhang, N. Hogg, Proteomic methods for analysis of S-nitrosation, J. Chromatogr. B 851 (2007) 152–159.
[12] A.B. Seabra, A. Fitzpatrick, J. Paul, M.G. de Oliveira, R. Weller, Topically applied S-nitrosothiol-containing hydrogels as experimental and pharmacological nitric oxide donors in human skin, Br. J. Dermatol. 151 (2004) 977–983.
[13] S.M. Shishido, M.G. de Oliveira, Polyethylene glycol matrix reduces the rates of photochemical and thermal release of nitric oxide from S-nitroso-N-acetylcysteine, Photochem. Photobiol. 71 (2000) 273–280.
[14] T.P. Amadeu, A.B. Seabra, M.G. de Oliveira, A.M.A. Costa, S-nitrosoglutathione-containing hydrogel accelerates rat cutaneous wound repair, J. Eur. Acad. Dermatol. Venereol. 21 (2007) 629–637.
[15] T.P. Amadeu, A.B. Seabra, M.G. de Oliveira, A. Monte-Alto-Costa, Nitric oxide donor improves healing if applied on inflammatory and proliferative phase, J. Surg. Res. 149 (2008) 84–93.
[16] J.L. Georgii, T.P. Amadeu, A.B. Seabra, M.G. de Oliveira, A. Monte-Alto-Costa, Topical S-nitrosoglutathione-releasing hydrogel improves healing of rat ischaemic wounds, J. Tissue Eng. Regenerat. Med. 5 (2011) 612–619.
[17] F.S. Schanuel, K.S.R. Santos, A. Monte-Alto-Costa, M.G. de Oliveira, Combined nitric oxide-releasing poly (vinyl alcohol) film/F127 hydrogel for accelerating wound healing, Colloids Surf. B Biointerfaces 130 (2015) 182–191.
[18] M. Champeau, V. Póvoa, L. Militão, F.M. Cabrini, G.F. Picheth, F. Meneau, C.P. Jara, E.P. de Araujo, M.G. de Oliveira, Supramolecular poly (acrylic acid)/F127 hydrogel with hydration-controlled nitric oxide release for enhancing wound healing, Acta Biomater. 74 (2018) 312–325.
[19] R. Vercelino, T.M. Cunha, E.S. Ferreira, F.Q. Cunha, S.H. Ferreira, M.G. de Oliveira, Skin vasodilation and analgesic effect of a topical nitric oxide-releasing hydrogel, J. Mater. Sci. Mater. Med. 24 (2013) 2157–2169.
[20] K.F.S. Ricardo, S.l.M. Shishido, M.G. de Oliveira, M.H. Krieger, Characterization of the hypotensive effect of S-nitroso-N-acetylcysteine in normotensive and hypertensive conscious rats, Nitric Oxide 7 (2002) 57–66.
[21] C.P. de Oliveira, F.I. Simplicio, V.M. de Lima, K. Yuahasi, F.P. Lopasso, V.A. Alves, D.S. Abdalla, F.J. Carrilho, F.R. Laurindo, M.G. de Oliveira, Oral administration of S-nitroso-N-acetylcysteine prevents the onset of non alcoholic fatty liver disease in rats, World J. Gastroenterol. WJG 12 (2006) 1905–1911.
[22] C.P. Oliveira, V.A. Alves, V.M. Lima, J.T. Stefano, V. Debbas, S.V. Sá, A. Wakamatsu, M.L. Corrêa-Giannella, E.S. de Mello, S. Havaki, D.G. Tiniakos, E. Marinos, M.G. de Oliveira, D. Giannella-Neto, F.R. Laurindo, S. Caldwel, F.J. Carrilho, Modulation of hepatic microsomal triglyceride transfer protein (MTP) induced by S-nitroso-N-acetylcysteine in ob/ob mice, Biochem. Pharmacol. 74 (2007) 290–297.
[23] C.P. de Oliveira, V.M. de Lima, F.I. Simplicio, F.G. Soriano, E.S. de Mello, H.P. de Souza, V.A. Alves, F.R. Laurindo, F.J. Carrilho, M.G. de Oliveira, Prevention and reversion of nonalcoholic steatohepatitis in OB/OB mice by S-nitroso-N-acetylcysteine treatment, J. Am. Coll. Nutr. 27 (2008) 299–305.
[24] R. Vercelino, I. Crespo, G.F. de Souza, M.J. Cuevas, M.G. de Oliveira, N.P. Marroni, J. González-Gallego, M.J. Tuñón, S-nitroso-N-acetylcysteine attenuates liver fibrosis in cirrhotic rats, J. Mol. Med. 88 (2010) 401–411.
[25] R.S. de Fraga, V.R. Camacho, G. Souza, C.S. Cerski, J.R. de Oliveira, M.G. de Oliveira, M. Álvares-da-Silva, S-nitroso-N-acetylcysteine: a promising drug for early ischemia/reperfusion injury in rat liver, Transplant. Proc. 42 (2010) 4491–4495.
[26] G.F.P. de Souza, J.K. Yokoyama-Yasunaka, A.B. Seabra, D.C. Miguel, M.G. de Oliveira, S.R.B. Uliana, Leishmanicidal activity of primary S-nitrosothiols against Leishmania major and Leishmania amazonensis: implications for the treatment of cutaneous leishmaniasis, Nitric Oxide 15 (2006) 209–216.
[27] A.J. Cariello, G.F.P. de Souza, A.S. Foronda, M.C.Z. Yu, A.L. Hofling-Lima, M.G. de Oliveira, In vitro amoebicidal activity of S-nitrosoglutathione and S-nitroso-N-acetylcysteine against trophozoites of Acanthamoeba castellanii, J. Antimicrob. Chemother. 65 (2010) 588–591.
[28] V. Mokhtari, P. Afsharian, M. Shahhoseini, S.M. Kalantar, A. Moini, A review on various uses of N-acetyl cysteine, Cell J. (Yakhteh) 19 (2017) 11.
[29] Y.-L. Zhao, P.R. McCarren, K. Houk, B.Y. Choi, E.J. Toone, Nitrosonium-catalyzed decomposition of s-nitrosothiols in solution: a theoretical and experimental study, J. Am. Chem. Soc. 127 (2005) 10917–10924.
[30] J. Dorado, B. Dlugogorski, E. Kennedy, J. Mackie, J. Gore, M. Altarawneh, Decomposition of S-nitroso species, RSC Adv. 5 (2015) 29914–29923.
[31] B. Meyer, A. Genoni, A. Boudier, P. Leroy, M.F. Ruiz-Lopez, Structure and stability studies of pharmacologically relevant S-nitrosothiols: a theoretical approach, J. Phys. Chem. 120 (2016) 4191–4200.
[32] M.M. Veleeparampil, U.K. Aravind, C.T. Aravindakumar, Decomposition of S-nitrosothiols induced by UV and sunlight, Adv. Phys. Chem. (2009) 2009.
[33] S.C. Askew, D.J. Barnett, J. McAninly, D.L.H. Williams, Catalysis by Cu2+ of nitric oxide release from S-nitrosothiols (RSNO), J. Chem. Soc. Perkin Trans. 2 (1995) 741–745.
[34] M.G. de Oliveira, S.M. Shishido, A.B. Seabra, N.H. Morgon, Thermal stability of primary S-nitrosothiols: roles of autocatalysis and structural effects on the rate of nitric oxide release, J. Phys. Chem. 106 (2002) 8963–8970.
[35] S.D.M. Lourenço, M.G. de Oliveira, Topical photochemical nitric oxide release from porous poly (vinyl alcohol) membrane for visible light modulation of dermal vasodilation, J. Photochem. Photobiol. Chem. 346 (2017) 548–558.
[36] D.L.H. Williams, The chemistry of S-nitrosothiols, Acc. Chem. Res. 32 (1999) 869–876.
[37] A. Krężel, W. Bal, Contrasting effects of metal ions on S-nitrosoglutathione, related to coordination equilibria: GSNO decomposition assisted by Ni (II) vs stability increase in the presence of Zn (II) and Cd (II), Chem. Res. Toxicol. 17 (2004) 392–403.
[38] D.L.H. Williams, The mechanism of nitric oxide formation from S-nitrosothiols (thionitrites), Chem. Commun. (1996) 1085–1091.
[39] L. Grossi, P.C. Montevecchi, A kinetic study of S-nitrosothiol decomposition, Chem. European J. 8 (2002) 380–387.
[40] L. Grossi, P.C. Montevecchi, S. Strazzari, Decomposition of S-nitrosothiols: unimolecular versus autocatalytic mechanism, J. Am. Chem. Soc. 123 (2001) 4853–4854.
[41] I. Hornyák, K. Marosi, L. Kiss, P. Gróf, Z. Lacza, Increased stability of S-nitrosothiol solutions via pH modulations, Free Radic. Res. 46 (2012) 214–225.
[42] L. Heikal, G.P. Martin, L.A. Dailey, Characterisation of the decomposition behaviour of S-nitrosoglutathione and a new class of analogues: S-Nitrosophytochelatins, Nitric Oxide 20 (2009) 157–165.
[43] E.E. Moran, Q.K. Timerghazin, E. Kwong, A.M. English, Kinetics and mechanism of S-nitrosothiol acid-catalyzed hydrolysis: sulfur activation promotes facile NO+ release, J. Phys. Chem. B 115 (2011) 3112–3126.
[44] S.l.M. Shishido, A.B. Seabra, W. Loh, M.G. de Oliveira, Thermal and photochemical nitric oxide release from S-nitrosothiols incorporated in Pluronic F127 gel: potential uses for local and controlled nitric oxide release, Biomaterials 24 (2003) 3543–3553.
[45] M.A. Skeff, G.A. Brito, M.G. de Oliveira, C.M. Braga, M.M. Cavalcante, V. Baldim, R.C. Holanda-Afonso, C.M. Silva-Boghossian, A.P. Colombo, R.A. Ribeiro, S-nitrosoglutathione accelerates recovery from 5-fluorouracil-induced oral mucositis, PLoS One 9 (2014) e113378.
[46] A.M.A. de Menezes, G.F.P. de Souza, A.S. Gomes, R.F. de Carvalho Leitão, R. de Albuquerque Ribeiro, M.G. de Oliveira, G.A. de Castro Brito, S-nitrosoglutathione decreases inflammation and bone resorption in experimental periodontitis in rats, J. Periodontol. 83 (2012) 514–521.
[47] M.M.d.S.G. Simões, M.G. de Oliveira, Poly (vinyl alcohol) films for topical delivery of S-nitrosoglutathione: effect of freezing–thawing on the diffusion properties, J. Biomed. Mater. Res. B Appl. Biomater. 93 (2010) 416–424.
[48] R.H. Marcilli, M.G. de Oliveira, Nitric oxide-releasing poly (vinyl alcohol) film for increasing dermal vasodilation, Colloids Surfaces B Biointerfaces 116 (2014) 643–651.
[49] P.D. Wood, B. Mutus, R.W. Redmond, The mechanism of photochemical release of nitric oxide from S-nitrosoglutathione, Photochem. Photobiol. 64 (1996) 518–524.
[50] G.F.P. de Souza, M.G. de Oliveira, Intratablet S-nitrosation: a new approach for the oral administration of S-nitrosothiols as nitric oxide donors, J. Pharmaceut. Sci. 105 (2016) 359–361.
[51] D.L.H. Williams, A chemist's view of the nitric oxide story, Org. Biomol. Chem. 1 (2003) 441–449.
[52] J.T. Barry, D.J. Berg, D.R. Tyler, Radical cage effects: comparison of solvent bulk viscosity and microviscosity in predicting the recombination efficiencies of radical cage pairs, J. Am. Chem. Soc. 138 (2016) 9389–9392.
[53] A.B. Seabra, G.F.P. de Souza, L.L. da Rocha, M.N. Eberlin, M.G. de Oliveira, S-nitrosoglutathione incorporated in poly (ethylene glycol) matrix: potential use for topical nitric oxide delivery, Nitric Oxide 11 (2004) 263–272.
[54] M.D. Bartberger, J.D. Mannion, S.C. Powell, J.S. Stamler, K.N. Houk, E.J. Toone, S− N dissociation energies of S-nitrosothiols: on the origins of nitrosothiol decomposition rates, J. Am. Chem. Soc. 123 (2001) 8868–8869.
[55] I. Sliskovic, A. Raturi, B. Mutus, Characterization of the S-denitrosation activity of protein disulfide isomerase, J. Biol. Chem. 280 (2005) 8733–8741.
[56] J.R. Pawloski, D.T. Hess, J.S. Stamler, Export by red blood cells of nitric oxide bioactivity, Nature 409 (2001) 622.

[57] Y. Zhang, N. Hogg, The mechanism of transmembrane S-nitrosothiol transport, Proc. Natl. Acad. Sci. Unit. States Am. 101 (2004) 7891–7896.
[58] S.D. Barnett, C.R. Smith, C.C. Ulrich, J.E. Baker, I.L. Buxton, S-Nitrosoglutathione, Reductase underlies the dysfunctional relaxation to nitric oxide in preterm labor, Sci. Rep. 8 (2018) 5614.
[59] D. Giustarini, A. Milzani, R. Colombo, I. Dalle-Donne, R. Rossi, Nitric oxide and S-nitrosothiols in human blood, Clin. Chim. Acta 330 (2003) 85–98.
[60] E.S.M. Ng, Z.-J. Cheng, A. Ellis, H. Ding, Y. Jiang, Y. Li, M.D. Hollenberg, C.R. Triggle, Nitrosothiol stores in vascular tissue: modulation by ultraviolet light, acetylcholine and ionomycin, Eur. J. Pharmacol. 560 (2007) 183–192.
[61] J. Oszajca, G. Stochel, E. Wasielewska, Z. Stasicka, R.J. Gryglewski, A. Jakubowski, K. Cieślik, Cyanonitrosylmetallates as potential NO-donors, J. Inorg. Biochem. 69 (1998) 121–127.
[62] L. Grossi, Nitric oxide: probably the in vivo mediator of the Bisulfite's effects, J. Biosci. Med. 2 (2014) 1–6.
[63] D.J. Sexton, A. Muruganandam, D.J. McKenney, B. Mutus, Visible light photochemical release of nitric oxide from S-nitrosoglutathione: potential photochemotherapeutic applications, Photochem. Photobiol. 59 (1994) 463–467.